

Fluorophore-conjugated anti-CEA Antibody for the Intraoperative Imaging of Pancreatic and Colorectal Cancer

Sharmeela Kaushal · Michele K. McElroy ·
George A. Luiken · Mark A. Talamini · A. R. Moossa ·
Robert M. Hoffman · Michael Bouvet

Received: 16 May 2008 / Accepted: 16 June 2008 / Published online: 30 July 2008
© 2008 The Society for Surgery of the Alimentary Tract

Abstract

Introduction Colorectal and pancreatic cancers together comprise the third and fourth most common causes of cancer-related death in the United States. In both of these cancers, complete detection of primary and metastatic lesions at the time of surgery is critical to optimal surgical resection and appropriate patient treatment.

Materials and Methods We have investigated the use of fluorophore-labeled anti-carcinoembryonic antigen (CEA) monoclonal antibody to aid in cancer visualization in nude mouse models of human colorectal and pancreatic cancer. Anti-CEA was conjugated with a green fluorophore. Subcutaneous, orthotopic primary and metastatic human pancreatic and colorectal tumors were easily visualized with fluorescence imaging after administration of conjugated anti-CEA. The fluorescence signal was detectable 30 min after systemic antibody delivery and remained present for 2 weeks, with minimal in vivo photobleaching after exposure to standard operating room lighting. Tumor resection techniques revealed improved ability to resect labeled tumor tissue under fluorescence guidance. Comparison of two different fluorophores revealed differences in dose–response and photobleaching in vivo.

Conclusion These results indicate that fluorophore-labeled anti-CEA offers a novel intraoperative imaging technique for enhanced visualization of tumors in colorectal and pancreatic cancer when CEA expression is present, and that the choice of fluorophore significantly affects the signal intensity in the labeled tumor.

Keywords Pancreatic neoplasms · Colorectal neoplasms ·
Carcinoembryonic antigen · Fluorescent antibody technique ·
Nude mouse cancer models · Fluorescence-guided surgery

Introduction

Colorectal and pancreatic cancers together comprise the third and fourth most common causes of cancer-related

These data were presented at the Society for Surgery of the Alimentary Tract meeting as part of the Digestive Diseases Week, San Diego CA, May 21 2008.

Sharmeela Kaushal and Michele K. McElroy shared authorship.

Work supported in part by: Cancer Therapeutics Training Program (T32 CA121938) National Institutes of Health (CA109949-03) American Cancer Society (RSG-05-037-01-CCE).

S. Kaushal · M. K. McElroy · M. A. Talamini · A. R. Moossa ·
R. M. Hoffman · M. Bouvet (✉)
Department of Surgery,
University of California San Diego, Moores Cancer Center,
3855 Health Sciences Drive #0987,
La Jolla, CA 92093-0987, USA
e-mail: mbouvet@ucsd.edu

G. A. Luiken
OncoFluor, Inc., San Diego, CA, 1211 Alameda Blvd,
Coronado, CA 92118, USA

R. M. Hoffman
AntiCancer, Inc., San Diego, CA, 7917 Ostrow St,
San Diego, CA 92111, USA

death in the United States.¹ In both of these cancers, the complete detection of primary and metastatic lesions prior to and at the time of surgery is critical to optimal surgical resection and appropriate patient treatment. For patients with pancreatic cancer, the lethality of this disease is primarily related to its aggressive biology and the often late stage at which patients are diagnosed.² Current chemotherapeutic regimens available offer only modest improvement in disease-related survival.^{3,4} Curative resection at the time of surgery remains the most powerful determinant for patient outcomes.⁵

For colorectal cancers, the high mortality of this disease in the United States parallels a high cancer incidence.¹ These patients more often present with resectable disease⁶ and have more surgical options than patients with pancreatic cancer.^{7,8} Nevertheless, there remains in this patient population a clear advantage to complete resection of all primary and metastatic cancer at the time of surgery when clinically appropriate.^{9,10}

The carcinoembryonic antigen (CEA) was first described following immunization of xenogenic animals with human tumor tissue.¹¹ Early evaluation of human tissue specimens revealed positive CEA expression in multiple cancers arising from the endodermally-derived epithelium of the digestive tract¹² as well as in human embryonic gut, pancreas, and liver tissue.¹³ Although initially described with respect to adenocarcinoma of the colon,¹² CEA is often also expressed in pancreatic ductal adenocarcinoma.^{14,15} In clinical medicine, CEA is most commonly utilized as a serum marker in colorectal and pancreatic cancer as a part of both preoperative staging and to follow patient response to surgery and chemotherapy.^{16,17}

We report here a study evaluating the use of a fluorophore-labeled anti-CEA monoclonal antibody to aid in primary and metastatic cancer visualization in nude mouse models of human colorectal and pancreatic cancer.

Materials and Methods

Cell Culture The human pancreatic cancer cell lines MiaPaca-2, ASPC-1, BxPC-3, XPA-1, XPA-3, and XPA-4 were maintained RPMI (Gibco-BRL, Grand Island, NY) supplemented with 10% fetal calf serum (FCS; Hyclone, Logan, UT). The human pancreatic cancer cell lines CFPAC & Capan-1 were maintained in IMDM (Gibco-BRL) with 15% FCS (Hyclone). The human pancreatic cancer cell lines Panc-1 and FG and the human colorectal cancer cell lines HCT 116, HT-29, SW480, LS174T, LOVO, and SW948 were maintained in DMEM (Gibco-BRL) supplemented with 10% FCS (Hyclone). All media was supplemented with penicillin/streptomycin (Gibco-

BRL), L-glutamine (Gibco-BRL), MEM nonessential amino acids (Gibco-BRL), sodium bicarbonate (Cellgro, Herndon VA), and sodium pyruvate (Gibco-BRL). All cell lines were cultured at 37°C with 5% CO₂. The Colo4104 tumors were generated from liver metastasis tissue from a human colon cancer patient which was serially passaged subcutaneously in athymic (*nu/nu*) mice. The human pancreatic cancer cell lines XPA-1, XPA-3, and XPA-4 were a gift from Dr. Anirban Maitra at Johns Hopkins University.

Conjugation of Antibody to Fluorophore Monoclonal antibody specific for CEA was purchased from Biodesign International (Saco ME, Cat # H45655M). Control IgG antibody was purchased from R&D Systems (Minneapolis MN, Cat # 6-001-A). The antibodies were labeled with the AlexaFluor 488 (Molecular Probes, Eugene, OR) or Oregon Green (Molecular Probes) fluorophores according to manufacturer's instructions. Briefly, for AlexaFluor 488 conjugation, the monoclonal antibody was reconstituted at 2 mg/mL in 0.1 M sodium bicarbonate; 500 µL of the 2 mg/mL were added to the reactive dye for each conjugation. For Oregon Green conjugation, the monoclonal antibody was reconstituted at 5 mg/mL in dH₂O, and 200 µL of the 5 mg/mL solution were added to the reactive dye for each conjugation. The antibody-dye mixtures were allowed to incubate for 1 h at room temperature, then overnight at 4°C. The conjugated antibody was then separated from the remaining unconjugated dye on a purification column by centrifugation. Antibody and dye concentrations in the final sample were determined using spectrophotometric absorbance. For each conjugation, the molar ratio of fluorophore to antibody was 3–4 to 1.

In Vitro Fluorescence Imaging All cell lines were plated in 96-well plates at 5×10^4 cells per well. After 48 h culture in appropriate media, the cells were incubated with 1 µg of fluorophore-conjugated anti-CEA or control-conjugated IgG antibody for 4 h at 37°C, then washed three times with phosphate-buffered saline (PBS; Gibco-BRL). Cells were imaged with an inverted Nikon DE-300 microscope and Spot camera RD. The images were then analyzed for fluorescence intensity using Image J software (National Institute of Health, Bethesda MD).

Animal Care Athymic mice were maintained in a barrier facility on high efficiency particulate air (HEPA)-filtered racks. The animals were fed with autoclaved laboratory rodent diet (Teckland LM-485; Western Research Products, Orange, CA). All surgical procedures and intravital imaging were performed with the animals anesthetized by intramuscular injection of 0.02 mL of a solution of 50% ketamine, 38% xylazine, and 12% acepromazine maleate. All animal studies were conducted in accordance with UCSD animal

care protocols and the principles and procedures outlined in the NIH Guide for the Care and Use of Animals.

Subcutaneous Tumor Cell Implantation Human pancreatic and colorectal cancer cell lines were harvested by trypsinization and washed twice with serum-free medium. Cells (1×10^6 in 100 μL of serum-free media) were injected subcutaneously within 30 min of harvesting over the right flank in female *nu/nu* mice between 4 and 6 weeks of age. Subcutaneous tumors were allowed to grow for 7–14 days until they reached a diameter of 1–2 mm prior to the delivery of conjugated antibody.

Subcutaneous Passage of Colo4104 Tumor Small (1 mm^3) fragments of the initial tumor sample obtained from the liver metastasis of a patient with stage IV colorectal cancer were implanted subcutaneously in athymic *nu/nu* mice. The tumors were maintained by serial subcutaneous passage. For passage, animals were anesthetized as described and a small 1-cm incision was made over the left flank. The harvested tumor was divided into 1-mm^3 pieces and implanted subcutaneously into the anesthetized mouse as described.

Orthotopic Tumor Implantation Orthotopic human pancreatic cancer xenografts were established in nude mice by direct injection of BxPC-3 tumor cells into the pancreas. For pancreatic tumors, a small incision was then made in the right pararectal line through the skin and peritoneum. The tail of the pancreas was exposed and 1×10^6 cells mixed 1:1 with matrigel (BD Biosciences, Bradford MA) in 30 μL final volume were injected into the pancreas using a Hamilton syringe (Hamilton Co, Reno NV). For colorectal tumors, a midline abdominal incision was made and a small segment of bowel and mesentery were exposed. A single 1-mm^3 tumor fragment from the Colo4104 tumor was sutured to the mesenteric border of the bowel wall using 8–0 nylon surgical sutures.¹⁸ Peritoneum and skin were closed using 6–0 vicryl sutures. Orthotopic tumors were allowed to grow for 7–14 days prior to imaging.

Experimental Peritoneal and Mesenteric Metastasis Model For models of intra-abdominal metastasis, human pancreatic (ASPC-1) and primary colorectal cancer (Colo4104) cells were used. For ASPC-1 implants, the cells were harvested by trypsinization and washed three times in serum-free media. The cells were resuspended in serum-free media at $5 \times 10^6/\text{mL}$. A volume of 200 μL of the cell suspension was then injected directly into the peritoneal cavity within 30 min of harvesting. For Colo4104 implants, solid tumor was minced into small ($<1 \text{ mm}^3$ diameter) pieces and dispersed in serum-free media; 500 μL of the tumor suspension was injected into the peritoneal cavity within

30 min of tumor harvest. The implants were allowed to grow for 7–14 days prior to imaging.

Antibody Delivery One to 2 weeks after subcutaneous, orthotopic, or intraperitoneal tumor implantation, animals were given a single intravenous (i.v.) injection of either conjugated anti-CEA or conjugated control IgG antibody diluted in PBS to a final volume of 100 μL . All i.v. injections were done via the tail vein. For the dose–response experiment, the antibody dose ranged from 12.5 to 75 μg . For the in vivo time course, photobleaching, and tumor resection experiments, the dose given was 75 μg . For the time course study, the animals were anesthetized and imaged at 30, 60 min, 2, 6, 8, 24, 48 h, and 8 and 15 days after systemic antibody delivery. For all other experiments, the animals were anesthetized and imaged 24 h after administration of the antibody.

Photobleaching In vitro tumor cells in 96-well plates were stained with conjugated anti-CEA as described, then exposed to standard OR lighting for 24 h. The cells were imaged on the Nikon inverted fluorescence microscope after 1, 2, 3, 4, 5, 6, 7, 8, 9, and 24 h of light exposure. Subcutaneous tumors were implanted as previously described. After 24 h of systemic antibody delivery, the animals were anesthetized and their subcutaneous tumor was exposed. The tumors were exposed to standard OR lighting, and the tumors were imaged on the Olympus OV100 Small Animal Imaging System over time for 8 h.

Tumor Resection Animals bearing subcutaneous BxPC3 tumors were anesthetized as described, and their right flank was sterilized. The tumor was exposed and imaged under both standard bright field illumination and fluorescence imaging. All visible tumors were removed under standard bright field illumination using a Stereo Discovery V12 dissecting microscope (Carl Zeiss IMT Corp, Maple Grove MN), and the tumor bed was then imaged again under standard bright field illumination and fluorescence imaging. All residual fluorescent tumor tissue remaining after resection was documented. The presence of tumor within the resection tissue and resection bed was confirmed by histology.

Animal Imaging Mice were imaged using the Olympus OV100 Small Animal Imaging System (Olympus Corp, Tokyo Japan),¹⁹ containing an MT-20 light source (Olympus Biosystems, Planegg, Germany) and either the DP71 CCD camera (Olympus Corp, Tokyo, Japan) for qualitative color images of tumor implants or with the Hamamatsu monochrome camera (Hamamatsu Corp, Hamamatsu City Japan) for quantitative evaluation of fluorescence intensity. All images were processed for contrast and brightness and

analyzed with the use of Image J and Photoshop element-4 (Adobe Systems Inc, San Jose CA).

Histology Tumor samples were surgically removed en bloc with surrounding tissue following in vivo imaging. These tissue samples were then frozen in Tissue-Tek O.C.T. compound (Sakura Fintek, Torrance CA) and sectioned on a microtome. For tumors removed from conjugated CEA- or IgG-treated animals, 15-µm sections were prepared without fixation for fluorescence microscopy, and 8-µm sections were fixed and stained with H&E for standard light microscopy. The prepared slides were imaged using an inverted Nikon DE-300 fluorescent microscope and Spot camera RD. Images were processed for contrast and brightness with the use of Photoshop element-4 (Adobe Systems Inc, San Jose CA).

Human Tissue Array Evaluation The human tissue array was purchased from US Biomax, Inc (Rockwell MD). The tissue array as well as 8-µm thick sections from the positive (ASPC-1 and Colo4104 tumors) and negative (murine axillary lymph node) controls were first fixed in ice-cold acetone for 2 min. The slides were then air-dried and washed three times with PBS. The slides were next with 5% bovine serum albumin (BSA; Sigma-Aldrich, St Louis, MO) for 1 h at room temperature. The slides were again washed with PBS and then stained using 1 µg/mL AlexaFluor 488 conjugated anti-CEA or isotype-control IgG for 2 h at room temperature. The slides were then washed for a final time and imaged using the inverted Nikon DE-300 fluorescent microscope and Spot camera RD.

Results

In Vitro Expression of CEA

Of the human pancreatic cancer cell lines which were evaluated in vitro, 70% of the pancreatic cancer cell lines tested were positive for CEA-staining in culture. These cell lines included MiaPaca-2, FG, ASPC-1, BxPC-3, CFPAC, Panc-1, and Capan-1. The cell lines tested which did not express CEA included XPA-1, XPA-3, and XPA-4. Of the human colon cancer cell lines which were tested in vitro, 67% of the colon cancer cell lines expressed CEA as identified by antibody staining. These cell lines included LOVO, HCT-116, SW948, and LS174T. The cell lines which did not express CEA above background were HT-29 and SW480. For each cell line tested, the plated cells were incubated with AlexaFluor 488-labeled anti-CEA or IgG at 1 µg/well. Positive staining was indicated by fluorescence intensity above background staining with conjugated IgG (Table 1).

Table 1 CEA Expression In Vitro and In Vivo

Human pancreatic cancer cell lines		
In vitro	+	–
Mia Paca-2	x	
FG	x	
BxPC-3	x	
CFPAC	x	
Panc-1	x	
Capan-1	x	
XPA-1		x
XPA-3		x
XPA-4		x
In Vivo	+	–
ASPC-1	x	
BxPC-3	x	
CFPAC	x	
Panc-1	x	
Capan-1	x	
Human colon cancer cell lines		
In vitro	+	–
LOVO	x	
HCT-116	x	
SW948	x	
LS174T	x	
HT-29		x
SW480		x
In vivo	+	–
LS174T	x	
Colo4104	x	

Testing of human pancreatic and colon cancer cell lines for in vitro and in vivo expression. Ten human pancreatic cancer cell lines were tested for in vitro CEA expression. Of the ten lines tested seven (70%) were positive. Six human colon cancer cell lines were tested for in vitro CEA expression, of which four (67%) were positive. Seven pancreatic and one colon cancer cell line were tested in vivo, all of which were positive. In addition, the primary human colon cancer tissue Colo4104 was also positive for in vivo expression of CEA. “+”= positive CEA expression; “–”=negative CEA expression

Imaging of Subcutaneous Tumors with Fluorescent Anti-CEA Antibody

Multiple cell lines were also assayed for in vivo expression of CEA in a subcutaneous cancer model. The human pancreatic cancer cell lines ASPC-1, BxPC-3, CFPAC, Panc-1, and Capan-1 were implanted subcutaneously. In addition, one colon cancer cell line (LS174T) and a primary human colon cancer specimen (Colo4104) were also implanted subcutaneously. All tumors were allowed to grow for 7–14 days (three animals were implanted with each cell line). When the tumors had reached approximately 1–2 mm in diameter, the animals were each given a single 75-µg dose of AlexaFluor 488-conjugated anti-CEA (two animals) or IgG (one animal). All five pancreatic cancer cell lines implanted demonstrated positive in vivo binding

of CEA as did the colon cancer cell line and the primary human colon cancer specimen as determined by fluorescence intensity above background IgG (Table 1).

Immunofluorescence Staining of Tissue for Binding with Anti-CEA Antibody

Screening of normal human tissue samples for binding to conjugated anti-CEA antibody was achieved by using immunofluorescence staining of a human tissue array. This array contains two samples each of 19 different non-cancerous adult human tissues including: salivary gland, liver, small intestine, stomach, kidney, skeletal muscle, skin, heart, placenta, breast, cervix, uterus, spleen, lung, brain, thyroid, pancreas, ovary, and adrenal gland. Human tumor samples generated subcutaneously in nude mice from the pancreatic cancer cell line ASPC-1 and the primary human colon cancer specimen Colo4104 were also stained using the same protocol as positive controls, and mouse axillary lymph node tissue was included as a negative control. Both the ASPC-1 pancreatic tumor and the Colo4104 colon tumor yielded positive staining for CEA. In non-cancerous tissues, the majority of samples did not demonstrate binding of conjugated anti-CEA above our isotype-control IgG background. A low level of staining above background was present within the small intestine cervix. Notably, the pancreas did not demonstrate any binding of conjugated anti-CEA. Table 2 denotes the staining for all non-cancerous human tissue samples tested.

Imaging Orthotopic Tumors with Fluorescent Anti-CEA Antibody

Tumors implanted orthotopically into the mouse pancreas and colon were evaluated for improved imaging using conjugated anti-CEA. For orthotopic tumors in the pancreas, the human pancreatic cancer cell line BxPC-3 was used. For the colon, Colo4014 was used. Orthotopic pancreatic or colon tumor-bearing animals were given a single dose of AlexaFluor 488-conjugated anti-CEA or IgG by tail vein, 7–10 days after tumor implantation, and imaged under both brightfield and fluorescence illumination using the Olympus OV100 Small Animal Imaging System. Intravital fluorescence imaging revealed what appeared to be very small pancreatic tumors which were difficult to visualize using standard brightfield illumination, even at higher magnification (Fig. 1b,c). However, under fluorescence imaging, not only was the tumor easily visible, it was clear that the extent of tumor invasion was much greater than that appreciated initially under brightfield imaging (Fig. 1e,f). The tumors in the colon cancer-bearing animals were larger and were visible under both brightfield and fluorescence imaging but more clearly by fluorescence (Fig. 2b,c & e,f).

Table 2 CEA Expression in Adult Human Tissues

Tissue	Staining
Salivary gland	–
Liver	–
Small intestine	+/-
Stomach	–
Kidney	–
Skeletal muscle	–
Skin	–
Heart	–
Placenta	–
Breast	–
Cervix	+
Uterus	–
Spleen	–
Lung	–
Brain	–
Thyroid	–
Pancreas	–
Ovary	–
Adrenal Gland	–
ASPC-1 tumor ^a	+++
Colo4104 tumor ^a	++
Mouse axillary LN ^b	–

Staining of a tissue array of adult non-cancerous human tissues revealed a small amount of positive staining over background in cervix and small intestine tissues. In the small intestine the staining was primarily limited to cells on the mucosal surface of the bowel. In the cervix, the staining was primarily seen on the luminal surface of glandular structures. The positive controls ASPC-1 and Colo4104 revealed staining with conjugated anti-CEA both within the cytoplasm and on the cell membrane throughout the tumors.

^a Positive control

^b Negative control

The animals which received conjugated IgG showed no green fluorescence in either their pancreatic (Fig. 1d) or colon (Fig. 2d) tumors. Orthotopic tumor tissue was confirmed by H&E (data not shown).

Imaging Intraabdominal Disseminated Tumor with Fluorescent Anti-CEA Antibody

Experimental models of intraabdominal metastases of pancreatic and colorectal cancer were created to facilitate the evaluation of fluorophore-conjugated anti-CEA binding to these lesions in vivo. Animals received a single intraperitoneal injection of human pancreatic (BxPC-3) or colorectal (Colo4104 or LS174T) cancer cells and these cells were allowed to grow within the peritoneal cavity for 7 days. After 1 week, the animals were given a single 75 µg injection of AlexaFluor 488-conjugated anti-CEA or IgG by tail vein; 24 h later, the animals were imaged on the Olympus OV100 using both brightfield and fluorescence illumination. At the time of imaging these animals had developed very small peritoneal implants on the bowel

Primary Colon Tumor Imaged After Systemic Delivery of AlexaFluor 488-Conjugated anti-CEA or AlexaFluor 488-Conjugated IgG Control

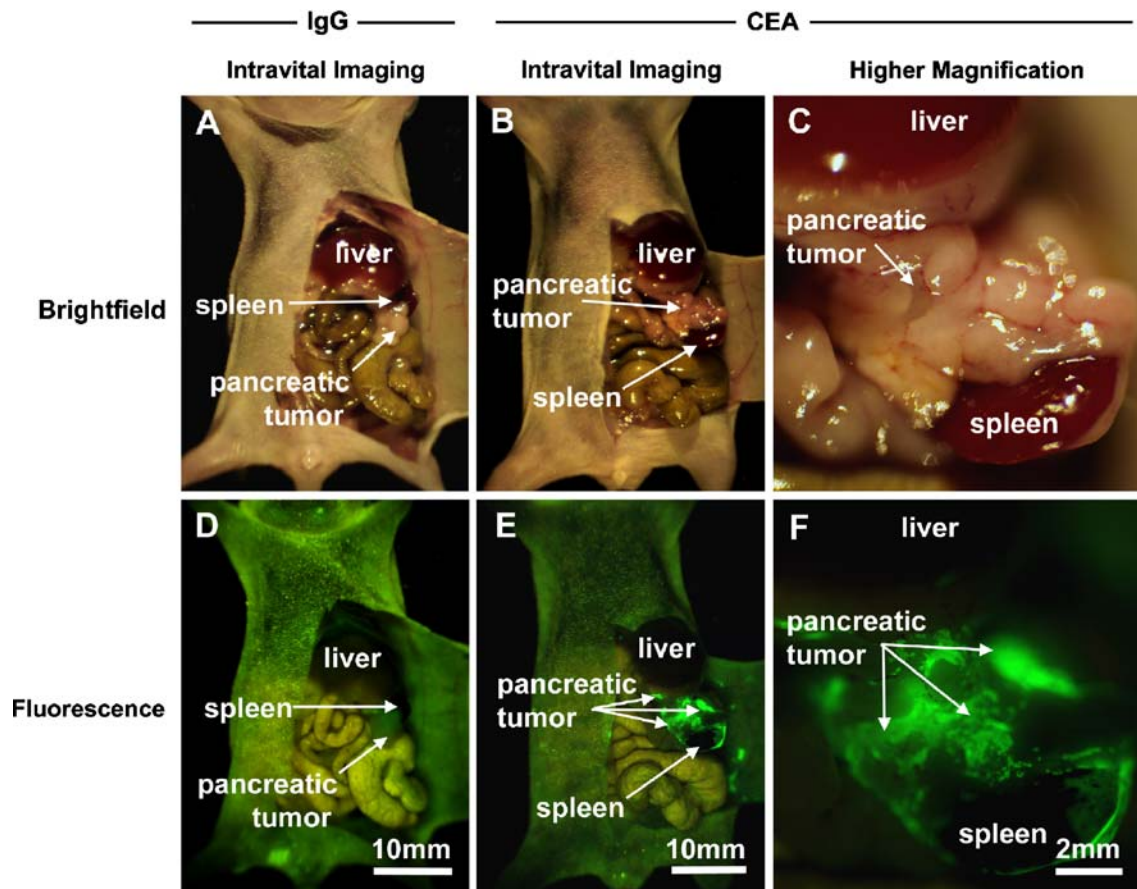


Figure 1 Imaging of orthotopic human pancreas tumors in vivo reveals greatly improved primary tumor visualization at laparotomy. Animals with orthotopically implanted BxPC-3 pancreatic tumors were imaged using both bright field (a–c) and fluorescence (d–f) illumination. Primary tumors were difficult to clearly discern under bright field imaging under both low (a, b) and high (c) magnification.

In contrast, fluorescence illumination of anti-CEA-labeled tumors revealed easy identification of primary tumor (e, f), which was much more extensive than initially appreciated. Animals given conjugated control IgG demonstrated no fluorescence signal in the orthotopic tumor (d). All tumor tissue was confirmed by histology; *n*=3.

and mesentery which were difficult to visualize using brightfield imaging (Figs. 3a,b and 4a,b) but were very clearly visible under fluorescence illumination in those animals given conjugated anti-CEA (Figs. 3c,d and 4c,d). The animals who received IgG had no discernible fluorescence signal in their tumor implants (data not shown).

Time Course Imaging of Pancreatic Tumors After Injection of Fluorescent Anti-CEA Antibody

Time-course evaluation of human pancreatic tumors in nude mice labeled with conjugated anti-CEA revealed rapid binding of the antibody-fluorophore conjugate in vivo with very long signal duration. Animals bearing 1–2-mm diameter subcutaneous ASPC-1 tumors were given a single dose of 75 µg AlexaFluor 488-conjugated anti-CEA by tail vein injection. The mice were then imaged at 30 min, 1, 2,

6, 8, 24, 48, 192 (8 days), and 360 h (15 days) after delivery of a single dose of antibody. Two animals were imaged for each time point. A small amount of fluorescence signal could be seen at 30 min post-antibody injection and the signal steadily increased to peak intensity at 24 h after injection. This signal remained relatively stable over the next 24 h and then decreased over the following 6 days to yield again a very low-level signal at 8 days post-injection. By 15 days post-injection, there was minimal signal remaining within the tumor tissue (Fig. 5).

Use of Fluorescent Anti-CEA Antibody to Image Post-resection Residual Tumor

In animals bearing larger (3–10 mm diameter) subcutaneous tumors, we investigated the use of fluorophore-conjugated anti-CEA to improve our ability to perform a

**Primary Colon Tumor Imaged After Systemic Delivery of
AlexaFluor 488-Conjugated anti-CEA or AlexaFluor IgG Control**

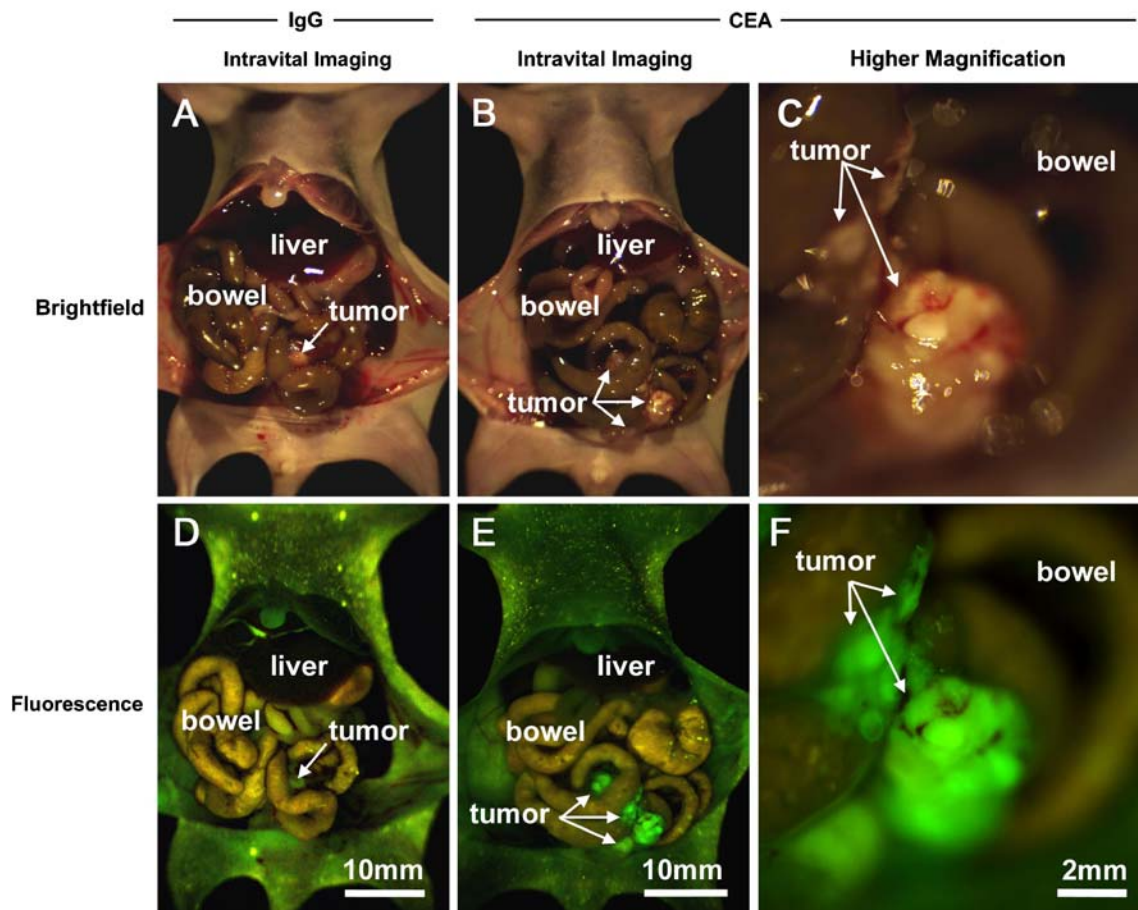


Figure 2 Imaging of orthotopic human colon tumors in vivo under fluorescence illumination improved primary tumor visualization at laparotomy. Animals with orthotopically implanted AC4104 colon tumors were imaged using both bright field (a–c) and fluorescence (d–f) illumination. Primary tumors labeled with conjugated anti-CEA

appeared bright green under fluorescence illumination (e, f). Animals given conjugated control IgG demonstrated no fluorescence signal in the orthotopic tumor (d). All tumor tissue was confirmed by histology; $n=3$.

complete tumor resection. Animals were given a single dose of AlexaFluor 488-conjugated anti-CEA 24 h prior to attempted surgical resection. At the time of surgery, animals were anesthetized and their tumors were imaged using brightfield and fluorescence illumination (Fig. 6a,b). The tumors were then carefully resected under a dissecting microscope under brightfield illumination with careful attention paid to removing all visible tumor tissue without adjacent normal skin or muscle (Fig. 6b,c). Following resection, the operative bed was then imaged using fluorescence microscopy and all remaining areas of fluorescence (Fig. 6e,f) were documented and biopsied. Of the three animals that underwent resection in this manner, all three had residual tumor present within the tumor bed which was not visible under brightfield illumination. The presence of tumor tissue within the resected tissue as well as the presence of tumor tissue

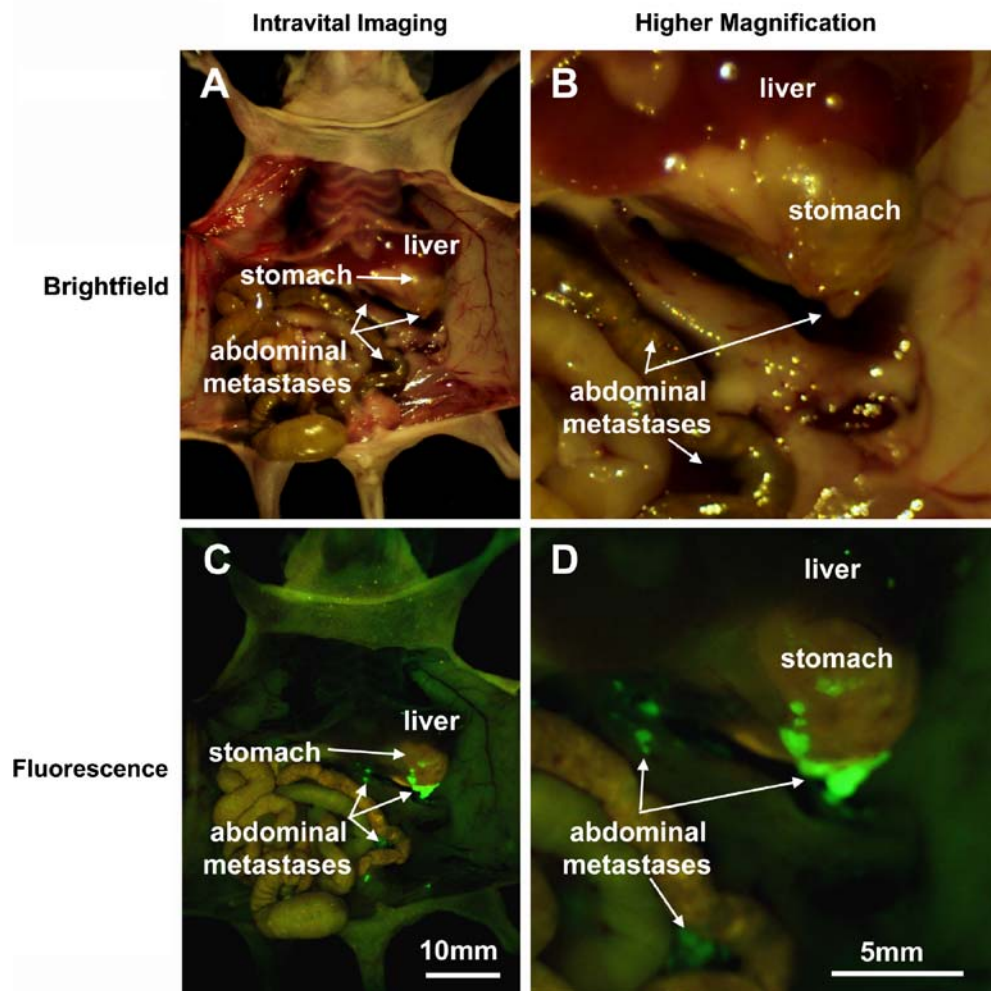
within the green fluorescent portions of the resection margin were confirmed by histology (data not shown).

Comparison of Fluorophores for Anti-CEA Antibody Conjugation

The choice of fluorophore can have a profound effect on fluorescence imaging in vitro and in vivo. For this reason, we elected to compare a commonly used green fluorophore, Oregon Green, to the AlexaFluor 488 fluorophore. We initially looked at anti-CEA conjugated with each of these fluorophores in an in vivo dosing experiment. Animals bearing 1–2-mm diameter subcutaneous ASPC-1 tumors were given a single administration of either AlexaFluor 488- or Oregon Green-conjugated anti-CEA in doses ranging from 12.5 to 75 μg by tail vein injection. 24 h after antibody delivery, the tumors were imaged using the

Figure 3 In vivo imaging of intraabdominal metastases from the human pancreatic cancer cell line BxPC-3 reveals greatly improved metastatic-tumor visualization at laparotomy. Animals with intraperitoneally injected BxPC-3 cells were imaged using both bright field (a, b) and fluorescence (c, d) illumination. Small metastatic implants on the bowel and mesentery were difficult to find with bright field imaging under both low (a) and high (b) magnification. In contrast, fluorescence illumination of anti-CEA-labeled tumors revealed easy identification of metastatic implants tumor (c, d); $n=3$.

Abdominal Pancreatic Metastases Imaged After Systemic Delivery of AlexaFluor 488-Conjugated Anti-CEA



Olympus OV100 Small Animal Imaging System. Three animals were evaluated at each dose for each fluorophore. Tumor fluorescence intensity increased for both fluorophores with increasing dose of fluorophore-conjugated antibody, as expected. The AlexaFluor 488-conjugated antibody showed a greater rate of in vivo fluorescence intensity increase at the three lower doses tested but demonstrated little increase from the 50 to 75 μg dose. Conversely, while the Oregon Green-conjugated antibody yielded greater in vivo fluorescence signal at the lowest dose tested, the signal remained lower than that for AlexaFluor 488 at all other doses (Fig. 7).

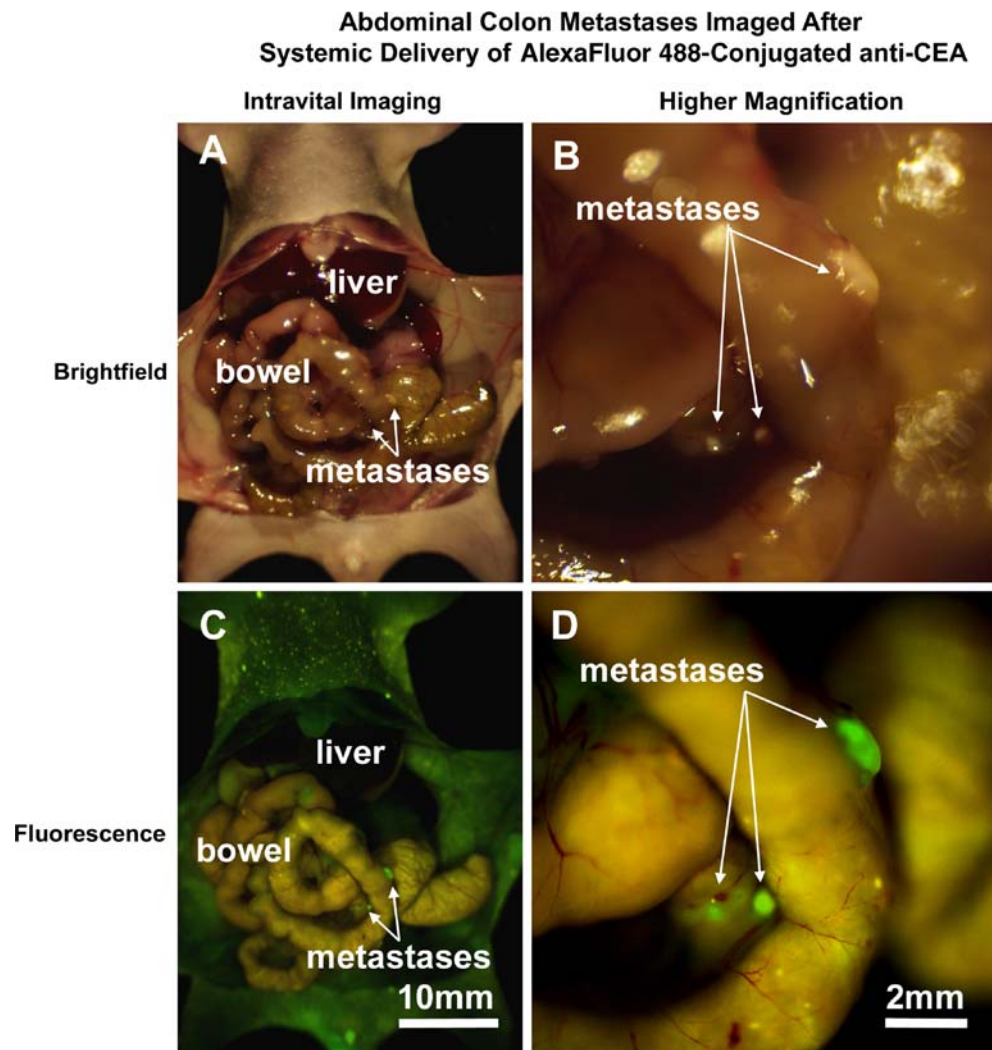
Photobleaching of Fluorophore-conjugated Anti-CEA Antibody

In a second comparison between AlexaFluor 488 and Oregon Green, we evaluated the propensity of these fluorophores to be affected by continuous bright-light illumination both in vitro and in vivo. Photobleaching is a

well-documented phenomenon in many fluorophores but is usually caused under conditions of laser excitation. It is unclear whether exposure to bright operating room (OR) lighting would cause any significant amount of fluorescence signal loss for either of these fluorophores. To evaluate this, we first looked in vitro at a confluent monolayer of ASPC-1 cells stained with either AlexaFluor 488-conjugated or Oregon Green-conjugated anti-CEA at 1 μg per well in triplicate in a 96-well plate. The cells were exposed to bright OR lighting for 24 h and were imaged each hour for the first 9 h and again at 24 h by fluorescence microscopy. The intensity of the fluorescence signal did decrease over the first 8 h by approximately 10% in the AlexaFluor 488-stained cells and by over 50% in the Oregon Green-stained cells. After 24 h, this had progressed to a 45% loss of fluorescence signal in the AlexaFluor group and a 67% loss for Oregon Green (Fig. 8a).

In vivo photobleaching was also evaluated using a subcutaneous tumor model. Nude mice bearing 1–2-mm diameter subcutaneous ASPC-1 tumors were given a single

Figure 4 Imaging of metastatic human colon tumors in vivo reveals improved tumor visualization at laparotomy. Animals with intraperitoneally injected Colo4104 colon cancer cells were imaged using both brightfield (a, b) and fluorescence (c–f) illumination. The metastatic implants were small and difficult to clearly discern under brightfield imaging under both low (a) and high (b) magnification. In contrast, fluorescence illumination of anti-CEA-labeled tumors revealed facile identification of metastases (c, d); $n=3$.



dose of 75 μg AlexaFluor 488- or Oregon Green-conjugated anti-CEA by tail-vein injection (three animals were included in each group). Twenty-four hours after antibody delivery, the animals were anesthetized and their subcutaneous tumor exposed to bright OR lighting via the excision of a small patch of overlying skin. The animals were imaged on the Olympus OV100 at 0, 2, 4, 6, and 8 h after exposure of the tumors to light. The amount of signal loss in vivo was much lower than that seen in cultured cells. Over an 8-h period, the AlexaFluor 488-labeled tumors lost

about 10% fluorescence signal while the Oregon Green-labeled tumors lost approximately 20% of their baseline fluorescence intensity (Fig. 8b). In both experiments, the amount of photobleaching observed was greater in the Oregon Green group.

Figure 5 Evaluation of fluorescence signal duration in subcutaneous ASPC-1 tumors following a single administration of AlexaFluor 488-conjugated anti-CEA reveals a rapid onset and prolonged duration of the in vivo fluorescence signal. Animals with small subcutaneous tumors were given a single dose of conjugated antibody and imaged at 30 min, 1, 2, 6, 8, 24, and 48 h, and 8 and 15 days after antibody administration. The fluorescence signal can be seen at 30 min and reaches its peak at 24 h after injection. The signal remains high at 48 h but by 8 days (192 h) after delivery has decreased to levels comparable to that seen at 30 min and by 15 days (360 h) was comparable to background; $n=18$.

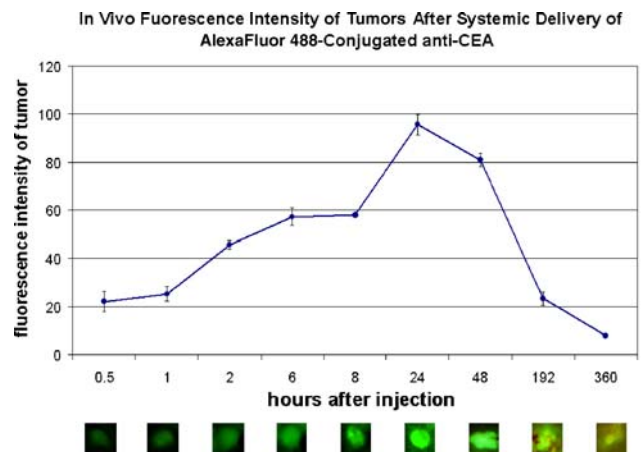
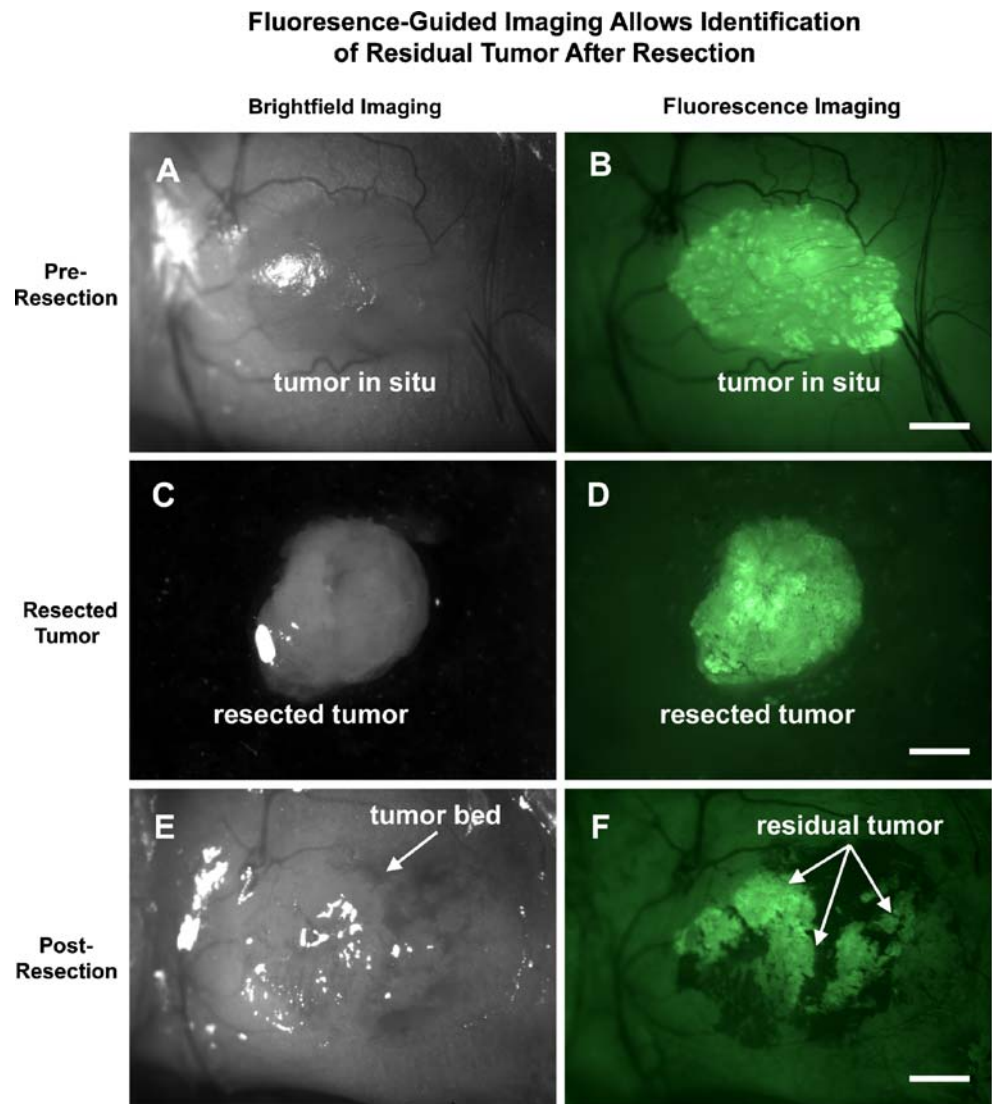


Figure 6 Tumor resection under bright-light microscopy. Larger subcutaneous AlexaFluor 488-conjugated anti-CEA-labeled BxPC-3 tumors were imaged under a dissecting microscope via both brightfield (a) and fluorescence (b) illumination. Under brightfield microscopy all visible tumor was resected, and the ex-vivo tumor was imaged under bright field (c) and fluorescence (d) microscopy. The tumor resection bed (e) was then imaged under fluorescence microscopy for any evidence of residual fluorescence (f). In all animals resected, there was residual tumor based on positive fluorescence signal within the tumor bed. Resected and residual tumor was confirmed by histology. All images taken at 20 \times , scale bars=1 mm; $n=3$.



Discussion

Targeted tumor imaging techniques are of great interest currently as we seek to improve our ability to localize and therefore appropriately treat the cancer burden in our patients. Fluorophore-conjugated antibodies, because they utilize technologies that have already been shown to be safe and efficacious in humans, present a unique opportunity to deliver highly specific fluorescence signals to the tissues of interest with minimal risk to patients. Monoclonal antibodies have been used safely in patients for some time,²⁰ as have several different fluorophores including fluorescein,^{21,22} a compound very similar to Oregon Green.²³ We sought to combine the specificity of a monoclonal antibody to a tumor-associated antigen with the enhanced imaging technologies afforded by fluorescence illumination to improve cancer imaging. In our nude mouse models of human pancreatic and colon cancer, the administration of conjugated anti-CEA improved our ability to visualize both

primary tumor as well as small intraabdominal lesions that were almost impossible to see under standard white light illumination even at high magnification.

In this study, we have investigated the use of fluorophore-conjugated anti-CEA for the in vivo imaging of pancreatic and colorectal cancer. The human carcinoembryonic antigen has been used clinically for many years to stage and follow patients with colorectal cancer.^{16,17} This tumor-associated antigen is strongly positive in virtually all colon cancers^{24,25} and up to 98% of pancreatic ductal adenocarcinomas.^{14,15} The lower percentage of established colorectal and pancreatic cancer cell lines expressing CEA in vitro likely reflects changes in antigen expression after prolonged maintenance in culture. It would be expected that prior histology studies reporting the proportion of primary pancreatic and colorectal cancers with CEA expression would more accurately reflect the likelihood of CEA expression in human tumors. Several groups have looked at the use of CEA expression for the identification of occult tumor cells in distant sites including

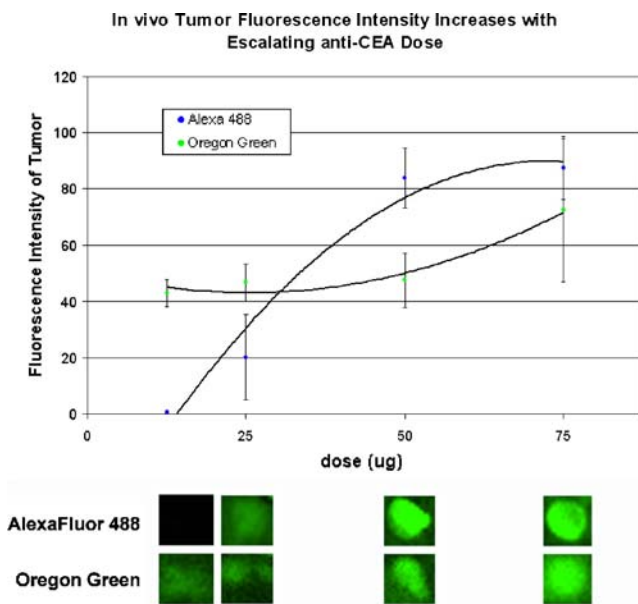


Figure 7 Dose response in vivo was compared for AlexaFluor 488-conjugated anti-CEA versus Oregon Green-conjugated anti-CEA. Animals bearing small subcutaneous ASPC-1 tumors were given doses of either AlexaFluor 488- (blue circles, upper pictures) or Oregon Green (green circles, lower pictures)-conjugated anti-CEA ranging from 12.5 µg to 75 µg per animal; 24 h after antibody delivery, the animals were imaged on the OV100. Although the Oregon Green-labeled tumors showed greater in vivo fluorescence intensity at the lowest dose (12.5 µg), the AlexaFluor 488-labeled tumors were brighter at the remaining doses (25, 50, and 75 µg); $n=12$ AlexaFluor 488, $n=12$ Oregon Green.

bone marrow, peripheral blood, and lymph nodes.²⁶ Kim et al. used CEA expression in liver metastases from primary colorectal cancer and found 100% of the metastatic implants tested expressed CEA.²⁷ Based on these data, we would expect a high proportion of metastatic lesions in patients with CEA-expressing primary tumors to also express this tumor-associated antigen.

Although there are some adult tissues which express a small amount of anti-CEA, including the colon, stomach, tongue, esophagus, and cervix,^{28,29} the level of expression in normal adult tissue is very low.^{14,30} In the case of intestinal expression of CEA, the signal is predominantly present on the luminal surface,^{14,30} and this non-tumor staining is unlikely to be great enough to obscure the signal from a CEA-expressing tumor. Our findings of weakly positive CEA staining only within the cervix and small intestine in our non-cancerous adult human tissue array parallels this previously published work. Although the tissue array used in our study did not contain a colon specimen, we expect that the CEA expression in colonic mucosa would also parallel historic reports. Given these findings, we expect that the use of this fluorophore-conjugated antibody would have relatively low non-tumor binding and thus low background fluorescence staining in patients.

One potential issue in the use of fluorescence imaging intraoperatively is the propensity of certain fluorophores to lose their fluorescence intensity with prolonged exposure to bright light, a phenomenon known as photobleaching.³¹ Due to differences between fluorophores in their signal intensity, photobleaching, and signal duration, it is of vital

In Vitro and In Vivo Photobleaching of anti-CEA-Stained ASPC-1 Cells

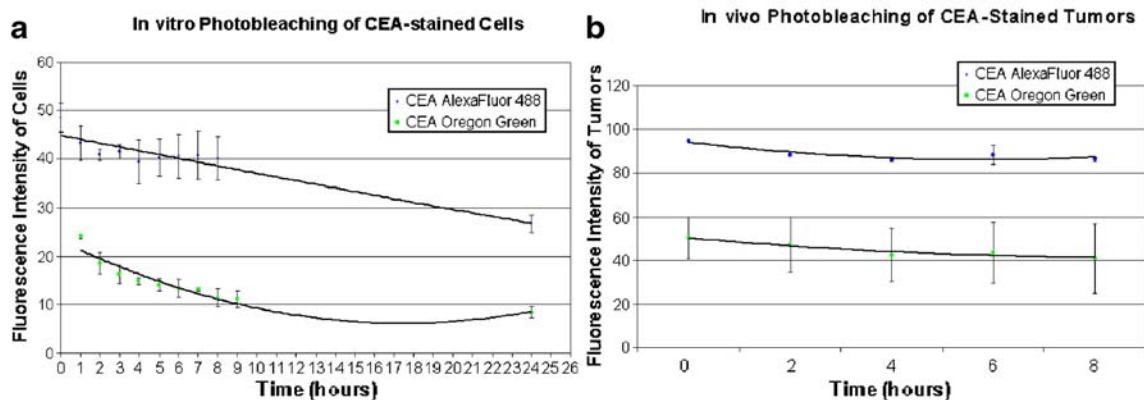


Figure 8 Both in vitro and in vivo photobleaching were compared for AlexaFluor 488- versus Oregon Green-labeled cells. In vitro AlexaFluor 488- and Oregon Green-stained ASPC-1 cells (a) were exposed to bright OR lighting for 24 h. The cells were imaged on a fluorescence microscope at 0, 1, 2, 3, 4, 5, 6, 7, 8, 9, and 24 h. The in vitro fluorescence signal in Oregon Green-labeled cells decreased by 50% and 67% at 9 and 24 h, respectively. AlexaFluor 488-stained cells lost only 10% and 45% of their signal at 9 and 24 h. In vivo

AlexaFluor 488- and Oregon Green-stained subcutaneous ASPC-1 tumors (b) were exposed to bright OR lighting for 8 h. The tumors were imaged on the OV100 at 0, 2, 4, 6, and 8 h. The in vivo fluorescence signal in Oregon Green-labeled tumors decreased by about 20% over 8 h, whereas that of the AlexaFluor 488-labeled tumors decreased by only 10%; $n=3$ AlexaFluor 488, $n=3$ Oregon Green.

importance to choose a stable fluorophore with appropriate signal intensity for in vivo use. We have compared two fluorophores, AlexaFluor 488 and Oregon Green, for their in vivo signal intensity and photobleaching kinetics under standard bright lighting compatible with OR lights. In our model, the AlexaFluor compound appeared to offer both a stronger and a more stable in vivo signal when compared to Oregon Green.

Several groups have recently looked at the use of fluorophore-conjugated monoclonal antibodies for the detection of tumor in animal models.^{32–35} Kulbersh and Withrow evaluated fluorescent-conjugated anti-EGFR and anti-VEGF respectively, in mouse models of head and neck cancer. Both groups found that the use of fluorophore-conjugated antibodies improved the sensitivity of tumor resection at surgery.^{33,34} Koyama et al. showed improved ability to image lung metastases using a rhodamine-conjugated antibody specific for Her2.³⁵ Hama et al. used a secondary antibody system in which the primary antibody, specific for Her1, was biotinylated. Mice bearing Her1-overexpressing intraabdominal tumors were given the biotinylated Her1 followed by a neutravidin-fluorescent conjugate to facilitate imaging of peritoneal tumor implants.³² We have previously described the use of fluorophore-conjugated CA19-9 in the evaluation of pancreatic cancer in a murine model system and found that the use of this antibody–fluorophore conjugate improved our ability to image orthotopic and metastatic pancreatic cancer.³⁶ CEA offers the advantage of being widely expressed in many gastrointestinal cancers and is frequently strongly positive in both pancreatic and colon cancer, with minimal expression in normal adult human tissues.

Limited studies have been done to date utilizing fluorescence technology to image tumor implants in human subjects. Fluorescence imaging has the potential for use in both laparoscopic and open surgery via either fluorescence laparoscopy or with the use of simple handheld LED lights and appropriate emission filters.³⁷ Fluorophore emissions can be affected by overlying tissue, with tissue absorption and scatter causing loss of the fluorescence signal. With respect to deep tumor deposits within solid organs such as the liver, the absorption and scatter of the fluorescence signal by the overlying tissue may hamper visualization of small lesions. For this reason, fluorescence-imaging techniques would best be paired with another method for evaluating deep tissue deposits such as intraoperative or laparoscopic ultrasound. Fluorescence laparoscopy following the pretreatment of tumor implants with sensitizing agents such as 5-aminolevulinic acid have been described in a small number of patients with encouraging improvements in the intraoperative localization of tumor implants.³⁸ The technology described here could easily be used intraoperatively either at staging laparoscopy, laparoscopic-

ic-assisted surgical resection, or even at laparotomy to improve not only detection of tumor metastases but also to facilitate the complete resection of the primary tumor.

Conclusions

In this study, we have used a fluorophore-antibody conjugate specific for the oncofetal antigen CEA to image both primary and metastatic colon and pancreatic tumors in mouse model systems. Our approach offers the advantage of a single antibody delivery and is very effective for imaging of primary and disseminated tumor. Fluorophore-conjugated anti-CEA improved visualization of primary and metastatic pancreatic and colorectal cancer and improved the identification of residual tumor tissue at the time of resection in a murine model. Fluorophore-conjugated anti-CEA has the potential to improve intraoperative visualization of both primary and metastatic pancreatic and colorectal cancer when CEA expression is present.

References

1. Jemal A, Siegel R, Ward E, Murray T, Xu J, Smigal C et al. Cancer statistics, 2006. *CA Cancer J Clin* 2006;56:106–30.
2. Wray CJ, Ahmad SA, Matthews JB, Lowy AM. Surgery for pancreatic cancer: recent controversies and current practice. *Gastroenterology* 2005;128:1626–41. doi:10.1053/j.gastro.2005.03.035.
3. Bria E, Milella M, Gelibter A, Cuppone F, Pino MS, Ruggeri EM et al. Gemcitabine-based combinations for inoperable pancreatic cancer: have we made real progress? A meta-analysis of 20 phase 3 trials. *Cancer* 2007;110:525–33. doi:10.1002/ncr.22809.
4. Boeck S, Ankerst DP, Heinemann V. The role of adjuvant chemotherapy for patients with resected pancreatic cancer: systematic review of randomized controlled trials and meta-analysis. *Oncology* 2007;72:314–21. doi:10.1159/000113054.
5. Wagner M, Redaelli C, Lietz M, Seiler CA, Friess H, Buchler MW. Curative resection is the single most important factor determining outcome in patients with pancreatic adenocarcinoma. *Br J Surg* 2004;91:586–94. doi:10.1002/bjs.4484.
6. Robinson MH, Thomas WM, Hardcastle JD, Chamberlain J, Mangham CM. Change towards earlier stage at presentation of colorectal cancer. *Br J Surg* 1993;80:1610–2. doi:10.1002/bjs.1800801241.
7. Pawlik TM, Schulick RD, Choti MA. Expanding criteria for resectability of colorectal liver metastases. *Oncologist* 2008;13:51–64. doi:10.1634/theoncologist.2007-0142.
8. Bonjer HJ, Hop WC, Nelson H, Sargent DJ, Lacy AM, Castells A et al. Laparoscopically assisted vs open colectomy for colon cancer: a meta-analysis. *Arch Surg* 2007;142:298–303. doi:10.1001/archsurg.142.3.298.
9. Turrini O, Viret F, Guiramand J, Lelong B, Bege T, Delperio JR. Strategies for the treatment of synchronous liver metastasis. *Eur J Surg Oncol* 2007;33:735–40. doi:10.1016/j.ejso.2007.02.025.
10. Andreoni B, Chiappa A, Bertani E, Bellomi M, Orecchia R, Zampino M et al. Surgical outcomes for colon and rectal cancer over a decade: results from a consecutive monocentric experience

- in 902 unselected patients. *World J Surg Oncol* 2007;5:73. doi:10.1186/1477-7819-5-73.
11. Gold P, Freedman SO. Demonstration of tumor-specific antigens in human colonic carcinomata by immunological tolerance and absorption techniques. *J Exp Med* 1965;121:439–62. doi:10.1084/jem.121.3.439.
 12. Gold P, Shuster J, Freedman SO. Carcinoembryonic antigen (CEA) in clinical medicine: historical perspectives, pitfalls and projections. *Cancer* 1978;42:1399–405. doi:10.1002/1097-0142(197809)42:3+<1399::AID-CNCR2820420803>3.0.CO;2-P.
 13. Gold P, Freedman SO. Specific carcinoembryonic antigens of the human digestive system. *J Exp Med* 1965;122:467–81. doi:10.1084/jem.122.3.467.
 14. Albers GH, Fleuren G, Escribano MJ, Nap M. Immunohistochemistry of CEA in the human pancreas during development, in the adult, chronic pancreatitis, and pancreatic adenocarcinoma. *Am J Clin Pathol* 1988;90:17–22.
 15. Yamaguchi K, Enji M, Tsuneyoshi M. Pancreatoduodenal carcinoma: a clinicopathologic study of 304 patients and immunohistochemical observation for CEA and CA19-9. *J Surg Oncol* 1991;47:148–54. doi:10.1002/jso.2930470303.
 16. Locker GY, Hamilton S, Harris J, Jessup JM, Kemeny N, Macdonald JS et al. ASCO 2006 update of recommendations for the use of tumor markers in gastrointestinal cancer. *J Clin Oncol* 2006;24:5313–27. doi:10.1200/JCO.2006.08.2644.
 17. Goldstein MJ, Mitchell EP. Carcinoembryonic antigen in the staging and follow-up of patients with colorectal cancer. *Cancer Invest* 2005;23:338–51.
 18. Fu XY, Besterman JM, Monosov A, Hoffman RM. Models of human metastatic colon cancer in nude mice orthotopically constructed by using histologically intact patient specimens. *Proc Natl Acad Sci USA* 1991;88:9345–9. doi:10.1073/pnas.88.20.9345.
 19. Yamauchi K, Yang M, Jiang P, Xu M, Yamamoto N, Tsuchiya H et al. Development of real-time subcellular dynamic multicolor imaging of cancer-cell trafficking in live mice with a variable-magnification whole-mouse imaging system. *Cancer Res* 2006;66:4208–14. doi:10.1158/0008-5472.CAN-05-3927.
 20. Reichert JM, Valge-Archer VE. Development trends for monoclonal antibody cancer therapeutics. *Nat Rev Drug Discov* 2007;6:349–56. doi:10.1038/nrd2241.
 21. Suzuki K, Kodama N, Sasaki T, Matsumoto M, Ichikawa T, Munakata R et al. Confirmation of blood flow in perforating arteries using fluorescein cerebral angiography during aneurysm surgery. *J Neurosurg* 2007;107:68–73. doi:10.3171/JNS-07/07/0068.
 22. Bartlett H, Eperjesi F. use of fundus imaging in quantification of age-related macular change. *Surv Ophthalmol* 2007;52:655–71. doi:10.1016/j.survophthal.2007.08.022.
 23. Hama Y, Urano Y, Koyama Y, Bernardo M, Choyke PL, Kobayashi H. A comparison of the emission efficiency of four common green fluorescence dyes after internalization into cancer cells. *Bioconjug Chem* 2006;17:1426–31. doi:10.1021/bc0601626.
 24. Itzkowitz SH, Shi ZR, Kim YS. Heterogeneous expression of two oncodevelopmental antigens, CEA and SSEA-1, in colorectal cancer. *Histochem J* 1986;18:155–63. doi:10.1007/BF01676115.
 25. Pihl E, McNaughtan J, Ward HA, Nairn RC. Immunohistological patterns of carcinoembryonic antigen in colorectal carcinoma. Correlation with staging and blood levels. *Pathology* 1980;12:7–13. doi:10.3109/00313028009060048.
 26. Tsavellas G, Patel H, Allen-Mersh TG. Detection and clinical significance of occult tumour cells in colorectal cancer. *Br J Surg* 2001;88:1307–20. doi:10.1046/j.0007-1323.2001.01863.x.
 27. Kim JC, Gong G, Roh SA, Park KC. Carcinoembryonic antigen gene and carcinoembryonic antigen expression in the liver metastasis of colorectal carcinoma. *Mol Cells* 1999;9:133–7.
 28. Prall F, Nollau P, Neumaier M, Haubeck HD, Drzeniek Z, Helmchen U et al. CD66a (BGP), an adhesion molecule of the carcinoembryonic antigen family, is expressed in epithelium, endothelium, and myeloid cells in a wide range of normal human tissues. *J Histochem Cytochem* 1996;44:35–41.
 29. Nap M, Mollgard K, Burtin P, Fleuren GJ. Immunohistochemistry of carcino-embryonic antigen in the embryo, fetus and adult. *Tumour Biol* 1988;9:145–53.
 30. Hammarstrom S. The carcinoembryonic antigen (CEA) family: structures, suggested functions and expression in normal and malignant tissues. *Semin Cancer Biol* 1999;9:67–81. doi:10.1006/scbi.1998.0119.
 31. Song L, Hennink EJ, Young IT, Tanke HJ. Photobleaching kinetics of fluorescein in quantitative fluorescence microscopy. *Biophys J* 1995;68:2588–600.
 32. Hama Y, Urano Y, Koyama Y, Choyke PL, Kobayashi H. Activatable fluorescent molecular imaging of peritoneal metastases following pretargeting with a biotinylated monoclonal antibody. *Cancer Res* 2007;67:3809–17. doi:10.1158/0008-5472.CAN-06-3794.
 33. Withrow KP, Newman JR, Skipper JB, Gleysteen JP, Magnuson JS, Zinn K et al. Assessment of bevacizumab conjugated to Cy5.5 for detection of head and neck cancer xenografts. *Technol Cancer Res Treat* 2008;7:61–6.
 34. Kulbersh BD, Duncan RD, Magnuson JS, Skipper JB, Zinn K, Rosenthal EL. Sensitivity and specificity of fluorescent immunoguided neoplasm detection in head and neck cancer xenografts. *Arch Otolaryngol Head Neck Surg* 2007;133:511–5. doi:10.1001/archotol.133.5.511.
 35. Koyama Y, Hama Y, Urano Y, Nguyen DM, Choyke PL, Kobayashi H. Spectral fluorescence molecular imaging of lung metastases targeting HER2/neu. *Clin Cancer Res* 2007;13:2936–45. doi:10.1158/1078-0432.CCR-06-2240.
 36. McElroy M, Kaushal S, Luiken GA, Talamini MA, Moossa AR, Hoffman RM, Bouvet M. Imaging of primary and metastatic pancreatic cancer using a fluorophore-conjugated anti-CA19-9 antibody for surgical navigation. *World J Surg* 2008;32:1057–1066.
 37. Yang M, Luiken G, Baranov E, Hoffman RM. Facile whole-body imaging of internal fluorescent tumors in mice with an LED flashlight. *Biotechniques* 2005;39:170–172.
 38. Zopf T, Schneider AR, Weickert U, Riemann JF, Arnold JC. Improved preoperative tumor staging by 5-aminolevulinic acid induced fluorescence laparoscopy. *Gastrointest Endosc* 2005;62:763–7. doi:10.1016/j.gie.2005.05.020.